ELSEVIER

Journal of Magnetism and Magnetic Materials 165 (1997) 149–152

journal of magnetism and magnetic materials

Observation of antiferromagnetic coupling in δ-MnGa/(Mn,Ga,As)/δ-MnGa trilayers

W. Van Roy [a,*], H. Akinaga [a,1], S. Miyanishi [a,b], K. Tanaka [a,b], L.H. Kuo [c]

[a] *Joint Research Center for Atom Technology, National Institute for Advanced Interdisciplinary Research, 1-1-4 Higashi, Tsukuba, Ibaraki 305, Japan*

[b] *Institute of Materials Science, University of Tsukuba, 1-1-1 Tennoudai, Tsukuba, Ibaraki 305, Japan*

[c] *Joint Research Center for Atom Technology, Angstrom Technology Partnership, 1-1-4 Higashi, Tsukuba, Ibaraki 305, Japan*

Abstract

We present the magnetic properties of δ-MnGa/(Mn,Ga,As)/δ-MnGa trilayers. The spacer layer consists of nominally 2 to 19 monolayers (ML) GaAs, but we have indications for an important incorporation of Mn and the possible formation of antiferromagnetic Mn_2As. Antiferromagnetic (AFM) coupling is observed for spacer layer thicknesses of 4 to 14 ML GaAs, ferromagnetic (FM) coupling exists outside this region. The largest observed coupling field was −87.0 mT (−870 Oe) at 17 K for a sample with a 12 ML spacer layer, causing a cross-over between both branches of the hysteresis loop and a negative remanence. In one sample (16 ML) the coupling changes from AFM at low temperature to FM at room temperature.

Keywords: Exchange coupling; Thin films – trilayer; Semiconductor spacer

The integration of ferromagnetic films with semiconductors has received increasing interest over the last years [1]. When the spacer layer in an exchange coupled multilayer is replaced by a semiconductor, coupling can be induced by heat [2] or light [3], and the giant magnetoresistance effect (GMR) increases with temperature [4]. Previously only the Fe/Si system has been studied [5]. We have recently succeeded in growing epitaxial δ-$Mn_{60}Ga_{40}$/(Mn,Ga,As)/δ-$Mn_{54}Ga_{46}$ trilayers on GaAs(001) using molecular beam epitaxy (MBE) [6]. δ-MnGa [7–9] is a ferromagnetic metal with a tetragonal crystal structure ($a = 2.72$ Å, $c = 3.58$–3.69 Å) and a strong magnetocrystalline anisotropy favoring the c-axis as magnetically easy axis. The bulk saturation magnetization at 0 K and the Curie temperature depend on the composition: $M_s = 450$–380 kA/m ($\mu_0 M_s = 0.57$–0.48 T) and $T_c \approx 327$–373°C for 56–59 at% Mn. Thin MnGa films can be grown epitaxially on GaAs(001) using MBE [10]. They have the c-axis perpendicular to the substrate, resulting in a perpendicular magnetic anisotropy and nearly square hysteresis loops. By choosing different compositions for the two MnGa films in our samples we obtain a different coercive field [11], which allows an easy identification of the various contributions to the magnetic hysteresis loops.

Regrowth of the GaAs spacer layer on top of MnGa was performed at a substrate temperature $T_{sub} = 300$°C by soaking the surface in As and depositing Ga in a pulsed way at a rate of 1 monolayer (ML) every 90 sec. Substrate temperatures above 350°C have resulted in surface degradation attributed to enhanced reactivity between MnGa and GaAs, causing the destruction of the MnGa film. Substrate temperatures of 250°C and lower suffer from three-dimensional nucleation and roughness due to insufficient surface mobility, and have so far resulted in a poor quality for the second MnGa film. Experiments to control the layer quality at reduced growth temperatures are in progress. At $T_{sub} = 300$°C the regrowth of GaAs results in a smooth surface with a streaky reflection high energy electron diffraction (RHEED) pattern. For regrowth thicknesses larger than nominally 14 ML there is a tendency for spots to appear, but this can be suppressed by decreasing the deposition rate to 1 ML every 120 or 150 s. However, we have indications that Mn is incorporated into the spacer layer, possibly up to several tens of at%, and that Mn_2As (or an intermediate phase between Mn_2As and GaAs) may be formed. Mn_2As is an antiferromagnetic metal with moments perpendicular to the c-axis and a Néel temperature $T_N = 300$°C [12,13]. It has a tetragonal unit cell with

* Corresponding author. Email vanroy@jrcat.or.jp; fax: +81-298-542786.

[1] Permanent address: Electrotechnical Laboratory, 1-1-4 Umezono, Tsukuba, Ibaraki 305, Japan.

PII S0304-8853(96)00491-X

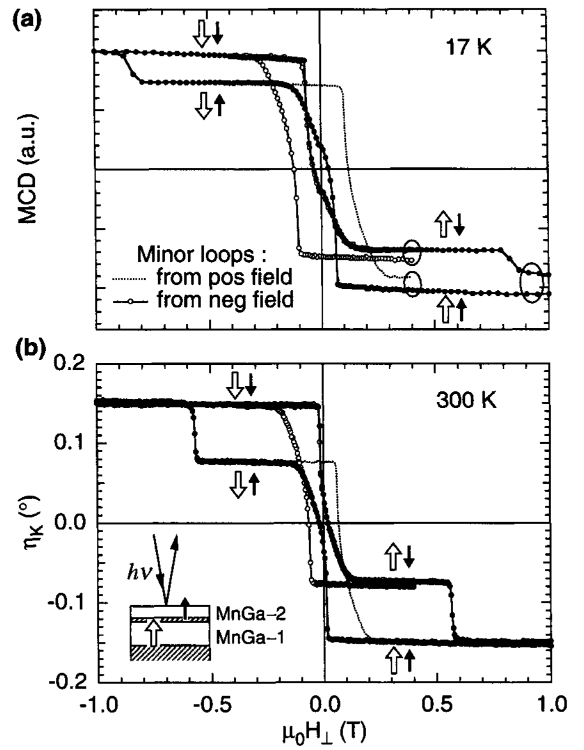

Fig. 1. Hysteresis loops of a sample with nominal structure 10 nm δ-$Mn_{60}Ga_{40}$/12 ML GaAs/20 nm δ-$Mn_{54}Ga_{46}$: (a) at 17 K (magnetic circular dichroism MCD at $h\nu = 3.70$ eV, the closing errors are due to condensation on the sample which changed the MCD amplitude); and (b) at room temperature (Kerr ellipticity at $h\nu = 3.70$ eV). The inset in (b) shows the measurement configuration. The minor loops where only the film with the lowest coercive field (20 nm $Mn_{54}Ga_{46}$) reverses are shifted by a field $\pm H_s$ depending on the magnetization of the second MnGa film (10 nm $Mn_{60}Ga_{40}$): (a) $\mu_0 H_s = -87.0$ mT (-870 Oe) at 17 K, and (b) $\mu_0 H_s = -39.0$ mT (-390 Oe) at room temperature. The coupling is antiferromagnetic in both cases. At 17 K the overall remanence of the sample is negative.

$a = 3.80$ Å and $c = 6.27$ Å. The presumed orientation is $[001]_{Mn_2As} \| [001]_{GaAs}$ and $[110]_{Mn_2As} \| [100]_{GaAs}$ and the lattice mismatch with GaAs and MnGa is -4.9% and -1.3%, respectively.

We now discuss a series of samples with nominal structure 10 nm $Mn_{60}Ga_{40}/n$ ML GaAs/20 nm $Mn_{54}Ga_{46}$/GaAs(001), where the nominal spacer layer thickness $n = 2$ to 19 ML GaAs. The magnetic properties are evaluated by perpendicular magneto-optic Kerr effect (MOKE) measurements at room temperature and by magnetic circular dichroism (MCD) measurements as a function of the temperature. All measurements were performed at a wavelength $\lambda = 335$ nm (3.70 eV). Fig. 1 shows the hysteresis loops for a sample with a nominally 12 ML GaAs spacer layer at 17 K (MCD) and 288 K (MOKE). Two steps can clearly be distinguished, corresponding to magnetization reversal of the individual MnGa films. Minor loops where only the magnetization of the low coercivity film reverses (= the bottom 20 nm $Mn_{54}Ga_{46}$ film) are shown as well. The second film (= the top 10 nm $Mn_{60}Ga_{40}$ film) remains fixed in the state that was set by a preceding large applied field. The minor loops are shifted along the field axis, the direction of the shift depending on the direction of magnetization of the high coercivity film. We define the coupling field H_s as the position of the center of the minor hysteresis loop when the hard MnGa film has a negative magnetization. A positive value for H_s indicates ferromagnetic (FM) coupling. For the sample shown in Fig. 1 the coupling is antiferromagnetic (AFM) with $\mu_0 H_s = -87.0$ mT (-870 Oe) at 17 K and $\mu_0 H_s = -39.0$ mT (-390 Oe) at room temperature. The estimated coupling energies are $J = \mu_0 M_{MnGa} t_{MnGa} H_s = -0.78$ and -0.35 mJ/m^2, respectively, using $t_{MnGa} = 20$ nm and $M_{MnGa} = 450$ kA/m (estimated from measurements on our single films [11]). It is interesting to note that the coupling field at 17 K is larger than the coercive field of the soft film, causing a magnetization reversal before the applied field is reduced to zero. Since the thickest film (20 nm) switches first, we observe a cross-over between both branches of the major hysteresis loop and a negative remanence at zero field.

The dependence of the coupling field H_s on the spacer layer thickness is shown in Fig. 2 (room temperature). We present the results versus the nominal thickness, as we have no verification of the spacer layer composition and effective thickness for all samples. The coupling is strong and AFM for thicknesses of 4 to 14 ML GaAs, and weaker FM outside this range. Due to the limited number of data points that are available it is not yet possible to determine whether the features in Fig. 2 represent a genuine thickness

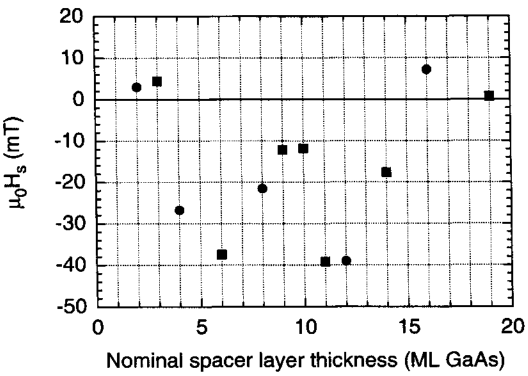

Fig. 2. Room temperature thickness dependence at of the coupling field H_s, determined from Kerr ellipticity hysteresis loops at $h\nu = 3.70$ eV. A positive value for H_s indicates ferromagnetic coupling. Strong antiferromagnetic coupling exists for nominal thicknesses in the range 4 to 14 ML GaAs, weaker ferromagnetic coupling is present outside this region. Squares and circles correspond to two sets of samples.

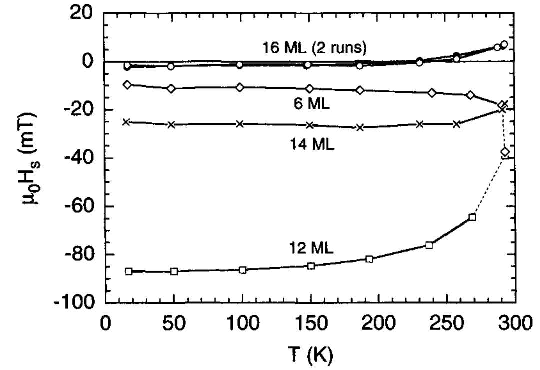

Fig. 3. Temperature dependence of the coupling field H_s, determined from MCD hysteresis loops at photon energy 3.70 eV. The results of room temperature Kerr ellipticity measurements are also shown (connected with a dotted line). For thick spacer layers (12, 14 and 16 ML GaAs) the coupling becomes more ferromagnetic with increasing temperature. In contrast, it becomes more antiferromagnetic for the sample with a thin spacer layer (6 ML). In one case (16 ML) there is a cross-over from antiferromagnetic to ferromagnetic coupling.

dependence, or if parasitic effects are present, such as changes in spacer layer structure or composition. The samples with the thinnest spacer layer (2 and 3 ML) still show separate steps in the hysteresis loop, indicating that both films reverse individually and that there is little or no direct FM bridging. The absence of bridging is also supported by the RHEED observations during the growth, where the pattern has already completely changed from the MnGa pattern to the typical pattern observed during spacer layer growth. The change to FM coupling for spacer layer thicknesses larger than 14 ML may be related to the tendency to spottiness that was observed in the RHEED pattern. In this thickness range it becomes difficult to maintain a good structural quality. Relaxation or phase separation may occur, influencing the magnetic properties.

Preliminary results for the temperature dependence of the coupling field have been obtained from MCD hysteresis loops using a closed cycle cryostat with a vacuum pressure in the 10^{-6} to 10^{-7} Torr range. Condensation on the sample surface caused a drift of the MCD amplitude, but this is a purely optical effect that did not interfere with the magnetic behavior. The steep magnetization reversal still allowed an accurate measurement of the coupling field H_s. The results for four of our samples are shown in Fig. 3. No universal trend can be distinguished. Depending on the sample the coupling field increases, decreases, or even changes sign with increasing temperature. In the three samples with a thick spacer layer (12, 14, and 16 ML) the coupling becomes more FM at higher temperature. In contrast, the coupling in the sample with a thinner spacer layer (6 ML) becomes more AFM. This suggests a competition between two or more coupling mechanisms with opposite sign and a different activation energy, which would explain also the sign change observed for one sample.

An in-depth discussion of the coupling mechanisms is beyond the scope of this paper. Here we present only some general considerations concerning the two main materials in our spacer layers. (1) Mn_2As has a layered antiferromagnetic structure perpendicular to the *c*-axis with a magnetic unit cell that is twice as high as the crystallographic one [13]. The orientation of the moments reverses three times within the crystallographic cell, which may cause thickness oscillations. Note, however, that in our samples the easy magnetic directions of MnGa ($\perp$) and Mn_2As ($\parallel$) are orthogonal to each other. The bulk Néel temperature $T_N = 300$°C suggests only a minor temperature dependence in the studied temperature range. However, in our samples T_N may be reduced due to the small film thickness or dilution with Ga, or enhanced by the proximity of MnGa. (2) Heavily doped degenerate semiconducting GaAs:Mn. The presence of magnetic moments inside the semiconductor may increase the coupling strength according to the model by Slonczewski [14], although in our case the biquadratic coupling predicted by this model would be suppressed by the strong uniaxial anisotropy of MnGa. In addition the Mn moments in the GaAs spacer may interact with each other, as in p-type $In_{0.987}Mn_{0.013}As$ where remanent magnetization is observed below $T_c \approx 7.5$ K [15]. Finally, an important aspect for semiconductor spacers is pinning of the Fermi energy E_f at the metal–semiconductor interfaces. In the case of GaAs pinning generally occurs close to mid-gap [16], which would result in an insulator-like behavior with a barrier height of $\sim E_g/2 = 0.71$ eV. Heavy Mn doping and a large defect density will result in band tails extending into the gap, an impurity band around the Mn level (0.095 eV above the valence band edge [17]) and defect states inside the gap, thus creating available states closer to E_f and reducing the temperature for thermal activation.

In summary, we have grown epitaxial MnGa/(Mn,Ga,As)/MnGa trilayers on GaAs(001). An important amount of Mn is believed to be included in the spacer layer, possibly also leading to the formation of antiferromagnetic Mn_2As. We observe a strong coupling between both ferromagnetic films. The coupling is AFM for nominal spacer layer thicknesses of 4 to 14 ML GaAs, and FM outside this range. No universal trend is found for the temperature dependence of the coupling field, suggesting a competition between two or more coupling mechanisms with different activation energy. The largest observed coupling field and energy were -87.0 mT and -0.78 mJ/m^2 for a 12 ML spacer layer at 17 K. This caused a cross-over between both branches of the major hysteresis loop and a negative overall remanence.

Acknowledgments. It is a pleasure to acknowledge Dr. T. Katayama and Dr. K. Ando (both at the Electrotechnical Laboratory) for the use of the MOKE and MCD setups. This work, partly supported by the New Energy and

Industrial Technology Development Organization (NEDO), was performed in JRCAT under the joint research agreement between NAIR and ATP.

References

[1] G.A. Prinz, Science 250 (1990) 1092.
[2] B. Briner and M. Landolt, Phys. Rev. Lett. 73 (1994) 340.
[3] J.E. Mattson, S. Kumar, E.E. Fullerton, S.R. Lee, C.H. Sowers, M. Grimsditch, S.D. Bader and F.T. Parker, Phys. Rev. Lett. 71 (1993) 185.
[4] K. Inomata, K. Yusu and Y. Saito, Jpn. J. Appl. Phys. 33 (1994) L1670.
[5] See also various papers in the Proceedings of the 40th Annual Conference on Magnetism and Magnetic Materials, Philadelphia, PA, 1995, J. Appl. Phys. 79 (1996) No. 8, Part 2A and 2B.
[6] W. Van Roy, H. Akinaga, S. Miyanishi, K. Tanaka and L.H. Kuo, Appl. Phys. Lett. 69 (1996) 711.
[7] T.A. Bither and W.H. Cloud, J. Appl. Phys. 36 (1965) 1501.
[8] M. Hasegawa and I. Tsuboya, Rev. Electric. Commun. Lab. 16 (1968) 605.
[9] X.-S. Lu, J.-K. Liang, T.-J. Shi and M.-G. Zhou, Acta Phys. Sinica 29 (1980) 469.
[10] M. Tanaka, J.P. Harbison, J. De Boeck, T. Sands, B. Philips, T.L. Cheeks and V.G. Keramidas, Appl. Phys. Lett. 62 (1993) 1565.
[11] W. Van Roy, H. Akinaga, S. Miyanishi and L. H. Kuo, unpublished.
[12] M. Yuzuri and M. Yamada, J. Phys. Soc. Japan 15 (1960) 1845.
[13] A.E. Austin, E. Adelson, and W. H. Cloud, J. Appl. Phys. 33 (1962) 1356.
[14] J.C. Slonczewski, J. Appl. Phys. 73 (1993) 5957; J. Magn. Magn. Mater. 150 (1995) 13.
[15] H. Ohno, H. Munekata, S. von Molnár and L.L. Chang, J. Appl. Phys. 69 (1991) 6103.
[16] S.M. Sze, Physics of Semiconductor Devices, 2nd ed. (Wiley, New York, 1981) pp. 276 and 291.
[17] S.M. Sze, Physics of Semiconductor Devices, 2nd ed. (Wiley, New York, 1981) p. 21.